Site-Directed Mutagenesis of Proline 52 To Glycine in Amicyanin Converts a True Electron Transfer Reaction into One that Is Conformationally Gated[†,‡]

John K. Ma,[§] Christopher J. Carrell,[||] F. Scott Mathews,[||] and Victor L. Davidson*[,§]

Department of Biochemistry, The University of Mississippi Medical Center, Jackson, Mississippi 39216-4505, and Department of Biochemistry and Molecular Biophysics, Washington University School of Medicine, St. Louis, Missouri 63110

Received March 14, 2006; Revised Manuscript Received May 16, 2006

ABSTRACT: Amicyanin is a type I copper protein that is the natural electron acceptor for the quinoprotein methylamine dehydrogenase (MADH). The conversion of Proline52 of amicyanin to a glycine does not alter the physical and spectroscopic properties of the copper binding site, but it does alter the rate of electron transfer (ET) from MADH. The values of electronic coupling (H_{AB}) and reorganization energy (λ) that are associated with the true ET reaction from the reduced *O*-quinol tryptophan tryptophylquinone (TTQ) of MADH to oxidized amicyanin are significantly altered as a consequence of the P52G mutation. The experimentally determined H_{AB} increases from 12 to 78 cm^{-1}, and λ increases from 2.3 to 2.8 eV. The rate and salt-dependence of the proton transfer-gated ET reaction from *N*-quinol MADH to amicyanin are also changed by the P52G mutation. Kinetic data suggests that a new common reaction step has become rate-limiting for both the true and gated ET reactions that occur from different redox forms of MADH. A comparison of the crystal structures of P52G amicyanin with those of native amicyanin free and in complex with MADH provided clues as to the basis for the change in ET parameters. The mutation results in the loss of three carbons from Pro52 and the movement of the neighboring residue Met51. This reduces the number of hydrophobic interactions with MADH in the complex and perturbs the protein−protein interface. A model is proposed for the ET reaction with P52G amicyanin in which the most stable conformation of the protein−protein complex with MADH is not optimal for ET. A new preceding kinetic step is introduced prior to true ET that requires P52G amicyanin to switch from this redox-inactive stable complex to a redox-active unstable complex. Thus, the ET reaction of P52G amicyanin is no longer a true ET but one that is conformationally gated by the reorientation of the proteins within the ET protein complex. This same reaction step now also gates the ET from N-quinol MADH, which is normally rate-limited by a proton transfer.

Amicyanin[1] from *Paracoccus denitrificans* is a cupredoxin that mediates the electron transfer (ET) from methylamine dehydrogenase (MADH) to cytochrome *c*-551i (*1*). Cupredoxins are a class of single-site type I blue copper proteins that mediate biological ET (*2*). These proteins exhibit molecular weights of 10−15 and overall structures that are primarily β-barrel. The most extensively studied cupredoxin has been azurin, which performs a general ET function in several bacteria (*2*). The overall secondary structure of amicyanin (*3*, *4*) is similar to that of azurin. Although both can be described as β-sandwich structures, azurin consists of eight strands with a small α-helical flap on the outside, and amicyanin consists of nine β-strands forming two mixed β-sheets. Whereas the copper center of oxidized amicyanin possesses four coordinating ligands, two N^{δ} of His95 and His53, sulfur of Cys92, and sulfur of Met98 at a longer distance forming a distorted tetrahedral geometry, azurin ligands consist of N^{δ} of two His residues, sulfurs of Cys and Met residues, and an additional axial ligand provided by the backbone carbonyl oxygen of a Gly residue to give it a trigonal bipyramidal geometry. The residue in amicyanin that corresponds in position in the structure of azurin to this Gly residue is Pro52. Because it is a proline, the orientation of its carbonyl oxygen is different, and it points away from the copper rather than providing a ligand. In this article, we investigated the consequences of changing Pro52 to Gly to see if the azurin copper geometry could be introduced into amicyanin.

MADH (*5*), amicyanin, and cytochrome *c*-551i (*6*) from *P. denitrificans* form one of the best characterized physiologic ET complexes of proteins. High resolution crystal structures are available not only for two of the individual proteins but also for the binary complex of MADH (*7*) and amicyanin and for a ternary protein complex (*8*), which includes cytochrome *c*-551i, the electron acceptor for ami-

[†] This work was supported by NIH Grant GM-41574 (to V.L.D.) and NSF Grant MCB0343374 (to F.S.M.).

[‡] Crystallographic coordinates have been deposited in the Protein Data Bank under file names 2GB2 (P52G Cu(II)) and 2GBA (P52G Cu(I)).

* To whom correspondence should be addressed. Email: vdavidson@biochem.umsmed.edu. Phone: 601-984-1516. Fax: 601-984-1501.

[§] The University of Mississippi Medical Center.

[||] Washington University School of Medicine.

[1] Abbreviations: MADH, methylamine dehydrogenase; TTQ, tryptophan tryptophylquinone; ET, electron transfer; H_{AB}, electronic coupling; λ, reorganization energy; E_m, oxidation−reduction midpoint potential; PT, proton transfer; DSC, differential scanning calorimetry; rmsd, root-mean-square difference.

10.1021/bi0605134 CCC: $33.50
Published on Web 06/16/2006

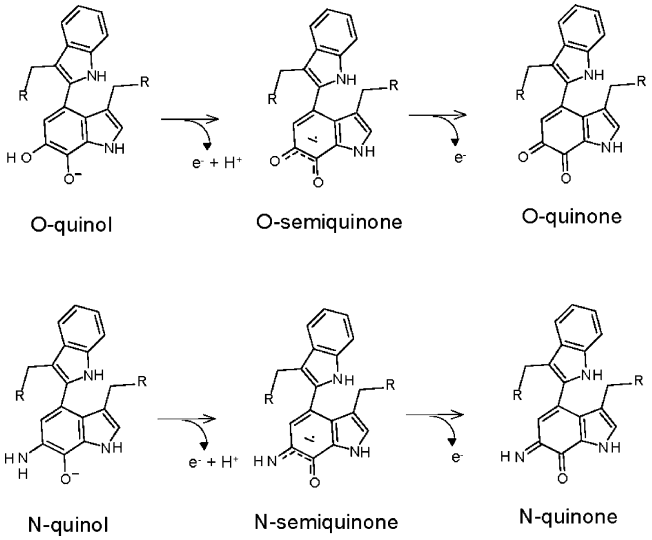

FIGURE 1: Different redox reactions of TTQ in methylamine dehydrogenase. The chemical reduction of MADH by dithionite yields the *O*-quinol form of TTQ. One electron oxidation of the *O*-quinol yields an *O*-semiquinone form of TTQ. A second one-electron oxidation yields the oxidized *O*-quinone TTQ. The reduction of MADH by the amine substrate yields an *N*-quinol form of TTQ in which the substrate-derived nitrogen has displaced the oxygen at the C6 position. One-electron oxidation of the *N*-quinol yields an *N*-semiquinone form of TTQ. A second one-electron oxidation yields an *N*-quinone TTQ, which may be then hydrolyzed to yield the *O*-quinone.

cyanin. Although MADH, amicyanin, and cytochrome *c*-551i are isolated as individual soluble proteins, they must form a complex in solution to catalyze the methylamine-dependent cytochrome *c*-551i reduction (*9*, *10*). Although it is a thermodynamically favorable reaction, MADH does not reduce cytochrome *c*-551i in the absence of amicyanin, probably because the proteins are unable to interact in a productive manner. Reduced amicyanin will not significantly reduce oxidized cytochrome *c*-551i in the absence of MADH at physiologic pH because the oxidation−reduction midpoint potential (E_m) value of free amicyanin is much more positive than that of the cytochrome at physiologic pH (*11*). The redox properties of amicyanin are altered on complex formation with MADH so as to facilitate the reaction by lowering the E_m value of amicyanin in complex under physiological conditions (*11*). This is because in reduced amicyanin, a pH-dependent conformational change occurs upon the protonation of the His95 copper ligand that exhibits a pK_a value of 7.7 (*11*). When protonated, His95 rotates 180° about its Cβ−Cγ bond, effectively removing it from the copper coordination sphere (i.e., flipped conformation). This conformational change is sterically restricted when amicyanin is in complex with MADH. This significantly lowers the pK_a value for this phenomenon, thus decreasing the E_m value of amicyanin at neutral pH when it is in complex with MADH.

ET between the tryptophan tryptophylquinone (TTQ) (*12*) prosthetic group of MADH and the type I copper center of amicyanin has been studied in solution by stopped-flow spectroscopy (*13*−*16*). It is possible to study ET from several different redox forms of MADH to amicyanin (Figure 1) (*17*). Because TTQ is a two-electron carrier and the type I copper is a one-electron carrier, two sequential oxidations of fully reduced TTQ by amicyanins are required to completely reoxidize MADH. The product of the reduction of MADH by the substrate amine is an *N*-quinol, which retains the covalently bound substrate-derived amino group after the release of the aldehyde product. An *N*-semiquinone is the product of the first one-electron oxidation of the *N*-quinol. The *O*-quinol and *O*-semiquinone forms of MADH may be generated by reduction with dithionite. The reactions of the *O*-quinol, *O*-semiquinone, and *N*-semiquinone forms of MADH with amicyanin exhibited a predictable dependence on $\Delta G°$. An analysis of the $\Delta G°$ dependence and temperature dependence of these ET reactions (*14*, *15*) yielded a reorganization energy (λ) value of 2.3 eV and an electronic coupling value (H_{AB}) of 12 cm^{-1}. These analyses also predicted an ET distance that approximated that seen in the crystal structure. In contrast, under physiological conditions, the reaction from *N*-quinol MADH to amicyanin is gated, and the observed rate is that of the deprotonation of the *N*-quinol amino group, which is dependent on the presence of monovalent cations (*16*, *18*). It was shown that during the reaction cycle of MADH, the protonated methylammonium substrate performs the role attributed to monovalent cations in vitro of regulating the rate and mechanism of ET from MADH (*19*).

This article describes the structure and physical and ET properties of P52G amicyanin. The results reveal unanticipated affects of the mutation on the ET reactions of P52G amicyanin. The ET results are interpreted in the context of the structure and physical properties as well as the kinetic models for the ET reactions. We concluded that the mutation of Pro52 alters the positions of residues that are involved in protein−protein interactions within the ET protein complex with MADH and consequently alters the kinetic mechanisms of the ET reactions from MADH to amicyanin. It is proposed that a conformational rearrangement of proteins within the complex is now required to poise the system for both the true ET reaction from the *O*-quinol TTQ and the gated ET reaction from the *N*-quinol TTQ. This new conformational rearrangement is a common rate-limiting step for the true and gated ET reactions from the different redox forms of MADH.

EXPERIMENTAL PROCEDURES

Protein Preparation. MADH (*20*) and amicyanin (*1*) were purified from *P. denitrificans* as previously described. Protein concentrations were calculated from the known extinction coefficients for oxidized amicyanin (ϵ_{595} = 4610 cm^{-1} M^{-1}) and oxidized MADH (ϵ_{440} = 26 200 cm^{-1} M^{-1}). *O*-Quinol MADH and reduced amicyanin were generated by titration of the oxidized proteins with stoichiometric amounts of dithionite. *N*-Quinol MADH is formed by the stoichiometric reduction by methylamine.

Site-directed mutagenesis to create P52G amicyanin was performed on double stranded pMEG201 (*21*), which contains the gene *mauC* (*22*) that encodes amicyanin, using two mutagenic primers with the QuikChange Site-Directed Mutagenesis Kit (Stratagene). The oligonucleotide sequences used to construct the site-directed mutant were 5′-CGCGAGGCGATGGGGCACAATGTCCATTTCG-3′and its complementary DNA. The underlined bases are those that were changed to create the desired change in the amino acid sequence. The entire 555-base *mau*C-containing fragment was sequenced to ensure that no second site mutations were

present, and none were found. P52G amicyanin was expressed in *E. coli* and purified from the periplasmic fraction as described for other recombinant amicyanin mutants (*21*).

X-ray Structure Determination. The P52G mutant crystals of amicyanin were grown by macroseeding, as described previously, using a 9:1 mixture of monobasic sodium (3 M) and dibasic potassium (3 M) phosphate solutions as precipitant (*23*). The crystals are monoclinic, space group $P2_1$, contain one molecule per asymmetric unit and are isomorphous with crystals of the wild-type protein. The cell dimensions are given in Table 1. X-ray diffraction data from the dark blue oxidized mutant crystals were recorded at the NE-CAT beamline 8-BM of the Advanced Photon Source using an ADSC-Q315 CCD detector. The data were recorded at 100 K, using paratone oil (Hampton Research, Laguna Hills, CA) as a cryoprotectant to 1.25 Å resolution (Table 1). Data were also recorded at 100 K using the same cryoprotection to 0.92 Å resolution from a colorless reduced-mutant crystal that had been incubated for ~30 min with 10 mM sodium ascorbate in 4 M sodium/potassium phosphate buffer in the ratio 4:1 (pH ~5.5) using the BIOCARS beamline 14-BM-C with an ADSC-Q4 CCD detector. Both data sets were processed using DENZO and SCALEPACK (*24*). The data collection statistics are presented in Table 1.

The structures of the oxidized and reduced forms of the P52G mutant were refined directly from the oxidized wild-type protein structures, after the prior removal of solvent molecules and alternate amino acid conformations, using SHELX (*25*). Alternating cycles of refinement and model building in XtalView were carried out. Hydrogen atoms, positioned as a riding model, were included in the refinements in SHELX. The temperature factors of all non-hydrogen atoms were refined anisotropically. The refinement statistics can be found in Table 1.

Modeling and Surface Area Calculations. Solvent accessibility and buried surface area (*22*) calculations were done using *Areaimol*, a part of the CCP4 crystallographic program suite (*26*). The modeling of the uncomplexed native and P52G mutant amicyanin structures into the ternary complex of MADH, amicyanin, and cytochrome *c*-551i (pdb ID, 2GC4)[2] was carried out by superimposing each amicyanin molecule onto the amicyanin portion of the complex using LSQMAN (*27*). In calculating the changes in the buried surface area caused by mutating Pro52 to Gly, atoms C_β, C_γ, and C_δ of Pro52 were deleted from the complex and the calculation of the change in accessible surface area repeated. This was done to eliminate changes in the buried surface area of the modeled complexes caused by side chain differences elsewhere from the mutation that would introduce systematic error into the calculations.

Spectrochemical Redox Potential Determination. The E_m values of P52G amicyanin free and in complex with MADH were determined by spectrochemical titration as described previously with the native proteins (*11*). The ambient potential was measured directly with a Corning combination redox electrode, which was calibrated using quinhydrone (a 1:1 mixture of hydroquinone and benzoquinone) as a standard with an E_m value of +286 mV at pH 7.0 (*28*).

For the determination of the E_m value of free amicyanin, the reaction mixture contained 365 μM amicyanin in 0.01 M bisTris propane (BTP) buffer at the indicated pH at 25 °C. Ferricyanide (400 μM) and quinhydrone (200 μM) were present as mediators. The mixture was titrated by the addition of incremental amounts of ascorbate, which was used as a reductant, and which had been previously adjusted to the set pH. The reaction was reversible. In the oxidative

Table 1: Data Collection and Refinement Statistics

sample	P52G Cu(II)	P52G Cu(I)
	Data Collection	
wavelength (Å)	0.9000	0.9000
space group	$P2_1$	$P2_1$
a (Å)	28.47	28.45
b (Å)	55.65	56.13
c (Å)	27.09	27.00
β (°)	95.08	96.98
max. resolution (outer shell) (Å)	1.25 (1.28−1.25)	0.92 (0.95−0.92)
I/σ(I) outer shell[a]	10.3 (2.8)	19.8 (4.5)
no. of observations	76798	110400
no. of unique reflections	21348	40193
percent completion (outer shell)	91.1 (52.4)	68.5 (50.7)
redundancy	3.6 (2.4)	2.7 (2.4)
R_{merge}[b] (outer shell)	0.101 (0.215)	0.037 (0.214)
	Refinement	
data range (Å)	30−1.25	30−0.92
no. of reflections	21277	39881
R_{work}[c]	0.130	0.108
R_{free}[c]	0.184	0.148
R_{total}[c]	0.133	0.111
no. of protein atoms	804	804
no. of copper ions	1	2
no. of solvent molecules	152	184
residues in alternate conformation	Val16	Glu84, His95, Cu^+
⟨B⟩ protein atoms (Å^2)[d]	19.5	10.8
⟨B⟩ anion atoms (Å^2)[d]	20.6	12.5
⟨B⟩ solvent atoms (Å^2)[d]	36.5	31.4
rms ΔB (m/m, Å^2)[d,e]	1.9	2.4
rms ΔB (m/s, Å^2)[d,e]	3.1	2.5
rms ΔB (s/s, Å^2)[d,e]	4.5	3.8
	Estimated Coordinate Error (Å)	
Luzzati[f]	0.155	0.127
DPI[g]	0.043	0.045

[a] I/σ(I) is the average signal-to-noise ratio for merged reflection intensities. [b] $R_{merge} = \Sigma_h\Sigma_I |I(h) - I_i(h)|/\Sigma_h\Sigma_i I_i(h)$, where $I_i(h)$ is the *i*th measurement, and $I(h)$ is the mean measurement of reflection *h*. [c] $R = \Sigma_h |F_o - F_c|/\Sigma_h |F_o|$, where F_o and F_c are the observed and calculated structure factor amplitudes of reflection *h*. R_{free} is the *R* for the test reflection data set (5% of the observed reflections) for cross validation of the refinement (*42*), R_{work} is the *R* for the working reflection set, and R_{total} is the *R* for all of the data. [d] The *B* values shown refer to the isotropic equivalent of the anisotropic thermal parameters used during the refinement. [e] Root-mean-square difference in the *B* factor for bonded atoms; m/m, m/c and c/c represent main chain−main chain, main chain−side chain, and side chain−side chain bonds, respectively. [f] Based on the Luzzati plot (*43*) of *R* vs 2 sin θ/λ, where θ is the angle of diffraction, and λ is the X-ray wavelength. [g] DPI is the diffraction-data precision indicator (*44*) based on *R* or R_{free} and is a rough approximation to the least-squares method.

[2] Chen, Z.-W., Durley, R., Davidson, V. L. and Mathews, F. S. Structural comparison of the oxidized ternary electron-transfer complex of methylamine dehydrogenase, amicyanin and cytochrome *c*-551i from *Paracoccus denitrificans* with the substrate-reduced, copper free complex at 1.9 Å resolution, unpublished work.

direction, the titration by the addition of potassium ferricyanide was performed. The absorption spectrum of amicyanin was recorded at different potentials, and the concentrations of oxidized amicyanin [Ami_{ox}] and reduced amicyanin [Ami_{red}] were determined by comparison with the spectra of the completely oxidized and reduced forms. The data were analyzed according to eq 1 to determine E_m values. The pK_a value was determined from the dependence of the E_m value of free amicyanin on pH according to eq 2.

$$E = E_m + (2.3RT/nF) \log ([Ami_{ox}]/[Ami_{red}]) \quad (1)$$

$$E_m = E_{m,7} - (2.3RT/nF) \log [(10^{-7} + K_a)/([H^+] + K_a)] \quad (2)$$

For the determination of the E_m value of P52G amicyanin in complex with MADH, the reaction mixture contained 20 μM amicyanin and 60 μM MADH in 0.01 M BTP at the indicated pH at 25 °C. Potassium ferricyanide (400 μM), quinhydrone (200 μM), and PES (40 μM) were present as mediators. The absorption spectrum of the complex was recorded at different potentials, and the concentrations of the oxidized and reduced forms were determined by comparison with the spectra of the completely oxidized complex and a mixture of oxidized MADH with fully reduced amicyanin. Data were then analyzed according to eq 1.

Differential Scanning Calorimetry. Solution DSC was performed, and the data was analyzed as described previously for native amicyanin (*29*) with a Calorimetry Sciences Corporation 6100 Nano II DSC with tantalum cells with a nominal volume of 0.33 mL. The buffer and the sample were scanned from 15 to 105 °C. As was reported for native amicyanin, it was not possible to obtain ΔH values for the calorimetric enthalpy of unfolding because of the irreversibility of the thermal denaturation, but it was possible to accurately determine T_m values, which define the midpoint temperature for the thermal transition.

EPR Spectroscopy. X-band EPR spectra were recorded on a Bruker E500 ELEXSYS spectrometer equipped with an Oxford Instruments helium flow cryostat at 10 K with a frequency of 9.633533 GHz, power of 0.02002 mW, modulation amplitude of 5 G, a modulation frequency of 100 kHz, a sweep time of 83.89 s, and a time constant of 81.92 ms. The protein sample contained 200 μM of P52G in 5% glycerol, 10 mM potassium phosphate at pH 7.4. Nine lines are accumulated.

Electron-Transfer Reactions of P52G Amicyanin. An On-Line Instruments (OLIS, Bogard, GA) RSM 16 stopped-flow rapid scanning spectrophotometer was used for the kinetic measurements. Experiments were performed in a 0.01 M potassium phosphate buffer at pH 7.5. The experimental details and methods of data analysis have been previously described (*30*, *31*).

To study the ET reaction from MADH to amicyanin, prior to mixing one syringe contained either reduced *O*-quinol or *N*-quinol MADH, whereas the other contained oxidized amicyanin. Pseudo-first-order conditions were maintained with excess amicyanin to MADH. ET reactions were fit to the simple kinetic model in eq 3 using eq 4, where A and B are the contents of the mixing syringes described above, and [S] refers to the concentration of the reagent, which is in excess and is varied to determine the concentration dependence of the observed rate (k_{obs}).

$$A_{ox} + B_{red} \overset{K_d}{\rightleftharpoons} A_{ox}/B_{red} \overset{k_3}{\underset{k_4}{\rightleftharpoons}} A_{red}/B_{ox} \quad (3)$$

$$k_{obs} = \frac{k_3[S]}{(K_d + [S]) + k_4} \quad (4)$$

Analysis of the Temperature Dependence of Reaction Rates. The temperature dependence of k_3 was analyzed according to ET theory (*32*) (eq 5 and eq 6). H_{AB} is the coupling constant, λ represents the reorganization energy, h is Plank's constant, T is temperature, R is the gas constant, and k_o is the characteristic frequency of nuclei (10^{13} s^{-1}), which is the maximum ET rate when the donor and acceptor are in van der Waals contact and $\lambda = -\Delta G°$.

$$k_{ET} = \frac{4\pi^2 H_{AB}^2}{h\sqrt{4\pi\lambda RT}} e^{\frac{-(\Delta G^0 + \lambda)^2}{4\lambda RT}} \quad (5)$$

$$k_{ET} = k_o \exp[-\beta(r - r_o)]\exp[-(\Delta G° + \lambda)^2/4\lambda RT)] \quad (6)$$

The donor to acceptor distance is r, and r_o is the close contact distance (3 Å). β is used to quantitate the nature of the intervening medium with respect to its efficiency to mediate ET. $\Delta G°$ is determined from the ΔE_m value for the reaction from eq 7.

$$\Delta G° = -nF\Delta E_m \quad (7)$$

RESULTS

Crystal Structure. The structure of the oxidized P52G mutant crystal was refined to near atomic resolution (1.25 Å) and that of the reduced mutant to atomic resolution (0.92 Å). An analysis of the structural quality of these crystals using PROCHECK indicates that all of the residues are in either the most favored or additionally allowed regions of the Ramachandran plot (*33*). The oxidized mutant structure exhibits alternate conformations for one side chain (Val16), whereas the reduced mutant exhibits alternate conformations for two side chains (Glu84 and His95) plus the copper ion.

The P52G oxidized structure is very similar to that of native amicyanin determined at 1.30 Å resolution (pdb ID, 1AAC). A comparison of Cα positions shows a rmsd between the two structures of 0.42 Å for all 105 residues. The largest deviations (>1.0 Å) occur at residues 18−20, a loop segment just before β-strand 2, known to be very flexible in amicyanin (*34*); the omission of these three residues leads to an rmsd of 0.26 Å for the remaining 102 residues. The electron density at residue 52 is consistent with the Pro to Gly mutation because all side chain density is absent. However, the backbone chain differs little in this region from native amicyanin, by less than 0.15 Å at positions 51−53; in particular, there is no structural rearrangement that would allow the carbonyl oxygen of Pro52 to form a fifth ligand to the copper atom. The conformation of the side chain of Met51 is also nearly the same in the mutant and in the native structure, with the S^{δ} atoms differing by only 0.8 Å in position. Also, there is little change in the solvent structure in this region.

The reduced P52G mutant is also very similar in structure to the native amicyanin, differing by 0.18 Å rmsd in Cα

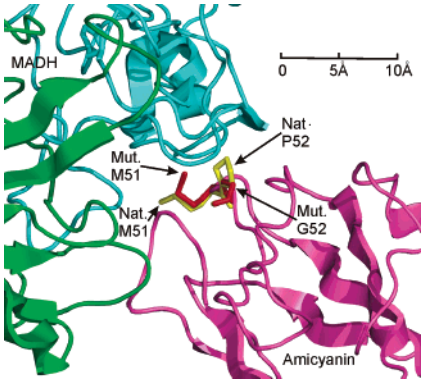

FIGURE 2: Changes in the structure and position of residues 51 and 52 at the MADH−amicyanin interface caused by the P52G amicyanin mutation. The structure of reduced P52G amicyanin was overlaid with that of amicyanin in the structure of the ternary protein complex with the MADH α-subunit in green, the *β*-subunit in blue, and the native amicyanin in violet, all shown as ribbons. Residues 51 and 52 of native amicyanin (Nat.) are colored yellow, and those residues in the P52G mutant amicyanin (Mut.) are colored red as indicated and are shown as sticks. The approximate scale of the diagram is also shown. This diagram was created using PYMOL (available on the world wide web at www.pymol.org).

position. This strong similarity extends to the oxidized mutant structure (rmsd = 0.49 Å overall, 0.27 Å omitting residues 18−20). Again, the main chain conformations of residues 51−53 in the reduced structure are similar to those of the native protein. However, the side-chain conformation of Met51 differs from that of native amicyanin so as to fold in more tightly toward residue 52 (Figure 2). In this configuration, the C^{ϵ} atom of Met51 would approach the proline side chain at position 52 by less than 3 Å, which would not be possible in the native structure. As discussed later, the different side-chain conformations of Met51 also affect its interaction with MADH.

The two conformations of the side chain of Val16 in the oxidized P52G structure and Glu84 in the reduced P52G structure each differ by a rotation about the Cα−C*β* bond (dihedral angle χ_1) by ∼120°; in each case, one of these configurations is close to that of the native protein (with an occupancy of about 0.7 and 0.4, respectively). His95 of the reduced P52G structure is in a flipped orientation (not coordinated to copper) about 50% of the time and in an unflipped orientation (coordinated to copper) the remainder of the time. The two positions of the copper ion are separated by 0.66 Å; the vector between them is nearly perpendicular to the plane defined by the copper ligands His53 ND1, Cys92 SG, and Met98 SD.

The two equally populated conformations of His95 and the copper ion of the reduced P52G structure correspond to tetrahedral and trigonal coordination geometries for the copper ion that differ in the presence (unflipped) or absence (flipped) of the His95 N^{ϵ} atom as a copper ligand. This situation (along with the corresponding geometries) is very similar to that observed in the crystal structure of the reduced wild-type amicyanin determined at 1.3 Å resolution (pdb ID, 2RAC) where both coordination states were found in approximately equal proportion (*11*). The latter structure was determined in a crystal that was equilibrated at pH 7.7 in the presence of excess ascorbate, and the equal distribution of states is consistent with the pK_a value of His95 in the wild-type structure. In the case of the P52G reduced structure, the crystal after reduction by ascorbate was maintained at about pH 5.5. Although this value is about 1 pH unit below that of the pK_a value of 6.3 observed for the P52G mutant in solution (discussed later), the observed distribution of conformers is not unreasonable, considering the presence of high salt and closely packed neighboring molecules in the crystal lattice.

Spectroscopic Properties. The spectroscopic properties of P52G amicyanin were very similar to those of native amicyanin. The visible absorption spectrum of oxidized P52G amicyanin (Figure 3A) is essentially identical to that of native amicyanin and exhibits a broad peak centered at 595 nm with an extinction coefficient of 4600 cm^{-1} M^{-1}. The EPR spectrum of oxidized P52G amicyanin (Figure 3B) is also indistinguishable from that of native amicyanin and is characteristic of a type 1 copper center with axial symmetry characterized by four hyperfine lines centered at $g_{||} = 2.24$ and separated by $A_{||} = 53$ G in the low magnetic field region with a center field of 3100 G and sweep width of 1500 G.

Stability. We have previously studied the stability of native amicyanin using solution DSC and demonstrated that the major thermal transition that occurs in the DSC profile correlates with disruption of the type I copper geometry (*29*). The T_m values for the major transitions of the oxidized and reduced forms of P52G amicyanin at pH 7.5 are 62.0 and 61.4 °C, respectively. These are very similar to the values obtained previously for native amicyanin of 63.0 and 62.6 °C, respectively, for the oxidized and reduced protein at pH 8.6, where the tetrahedral type I geometry is maintained in both redox states. At lower pH where the geometry of the reduced native amicyanin becomes trigonal planar, the oxidized form exhibits greater stability than the reduced one. These data indicate that P52G mutation has had little effect on the stability of amicyanin and suggest that both the oxidized and reduced forms of P52G amicyanin exhibit the same copper ligand geometry at pH 7.5.

Redox Properties. The redox properties of P52G amicyanin were examined by spectrochemical titration of the protein free and in complex with MADH (Table 2). The E_m value of free P52G amicyanin at pH 7.0 is about 50 mV less positive than that of native amicyanin. An analysis of the pH dependence of the E_m value revealed that this decrease at neutral pH is due primarily to a shift in the pK_a value from 7.7 to 6.3, rather than a change in the electronic properties of the copper center. The E_m value of native amicyanin in complex with MADH decreases on complex formation with MADH at pH 7.0 because the conformational change that is linked to the protonation of His95 is sterically restricted. Thus, native amicyanin in complex at pH 7.0 exhibits an E_m value similar to that of free amicyanin at pH values well above the pK_a value (*11*). The E_m value of P52G amicyanin in complex with MADH was determined to be approximately the same as that of free P52G amicyanin at pH 7.0, consistent with the finding that the pK_a of the E_m value is shifted to a more acidic value as a consequence of the mutation. The $\Delta G°$ values for the redox reactions between MADH and amicyanin were determined from the ΔE_m value for the reaction according to eq 7 using the previously determined E_m values for MADH (*35*). We have previously shown (*14*) that the E_m values of the native proteins and the $\Delta G°$ value for the reactions under study do not significantly change over the temperature range that is used in the ET studies described below.

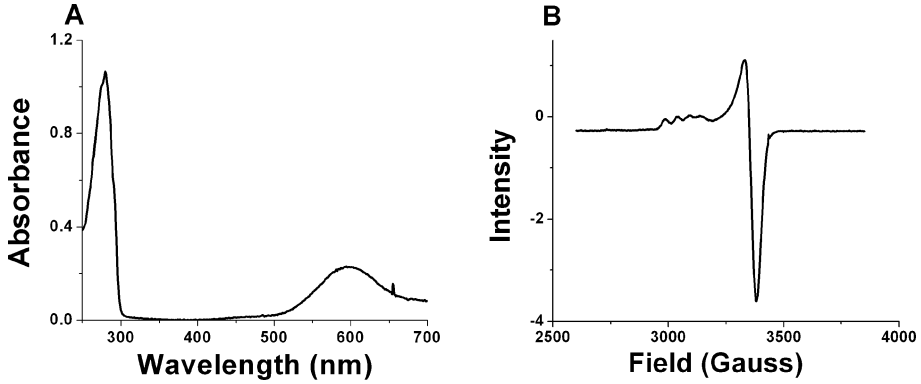

FIGURE 3: Spectroscopic properties of P52G amicyanin. (A) Visible absorption spectrum of oxidized P52G (45 μM) recorded in 10 mM potassium phosphate at pH 7.4. (B) X-band EPR spectrum of oxidized P52G amicyanin (200 μM) recorded in 10 mM potassium phosphate at pH 7.4 plus 5% glycerol.

Table 2: Redox Properties of Native and P52G Amicyanins Free in Solution or in Complex with MADH

	native amicyanin[a]	P52G amicyanin
$E_{m,7}$ (free)	+294 mV	+240 mV
pK_a (free)	7.7	6.3
$E_{m,7}$ (in complex)	+220 mV	+240 mV

Table 3: Electron Transfer Parameters for the Reactions of *O*-Quinol MADH with Native and P52G Amicyanins

parameters	native amicyanin[a]	P52G amicyanin
K_d (μM)	4.5 ± 0.5	38 ± 12
k_3 30°C (s^{-1})	10 ± 0.7	3 ± 0.3
$\Delta G°$ (J mol^{-1})[b]	−3184	−4824
λ (eV)	2.3 ± 0.1	2.8 ± 0.1
H_{AB} (cm^{-1})	12 ± 7	78 ± 34
r (Å)	9.5 ± 0.8	6 ± 0.9

[a] Taken from ref 13. [b] Values of $\Delta G°$ were determined from the ΔE_m values. The error in the measurement of the E_m values for each reactant is <5%.

ET from O-Quinol MADH to P52G Amicyanin. On the basis of the $\Delta G°$ values for the redox reaction, ET from *O*-quinol MADH to P52G amicyanin in complex is expected to be faster than that to native amicyanin. Instead, the k_3 value (eq 3) determined at 30 °C is significantly less than that of the native reaction (Table 3). The K_d value as determined from eq 4 has also increased approximately 7-fold. The k_3 values for the ET reaction from *O*-quinol MADH to oxidized P52G were determined over a range of temperatures from 15 to 42 °C. An analysis of these data by eq 5 (Figure 4 and Table 3) revealed that the values for both λ and H_{AB} that are associated with this reaction significantly increased. An analysis by eq 6 further indicated that, if this is a true ET reaction, then the ET distance is decreased by 3.5 Å relative to that of the reaction with native amicyanin. As discussed later, such a decrease in distance is not possible; therefore, the most likely explanation for these changes in ET parameters is that as a consequence of the P52G mutation the ET reaction is no longer a true ET reaction.

ET from N-Quinol MADH to P52G Amicyanin. It was previously shown that the ET reaction from *N*-quinol MADH to amicyanin is not a true ET reaction but one that is chemically gated (*36*) by a rate-limiting deprotonation of the *N*-quinol to generate an activated intermediate from which very rapid ET occurs (*16*, *18*, *19*). Thus, this reaction is much faster than the reaction of the *O*-quinol MADH, despite being a gated ET reaction. Interestingly, the k_3 value for the reaction of *N*-quinol MADH with P52G amicyanin determined at 30 °C is significantly less than that of the native reaction (Table 4) and similar to the value obtained for the reaction of *O*-quinol MADH with P52G amicyanin under similar conditions (Table 3). The limiting first-order rate constant for the gated ET reaction of *N*-quinol MADH with native amicyanin is strongly salt-dependent and increases dramatically from 0 to 400 mM KCl. This is because the rate-limiting proton transfer (PT) requires the presence of a monovalent cation at the active site (*18*). Therefore, the salt-dependence of k_3 for the reaction of *N*-quinol MADH with oxidized P52G amicyanin was examined (Table 4). The rate of the reaction of P52G amicyanin with *N*-quinol MADH is also salt-dependent but to a different extent than the reaction with native amicyanin. In contrast to the results obtained with native amicyanin, the rate of the reaction with P52G amicyanin increases and plateaus at about 150 mM KCl.

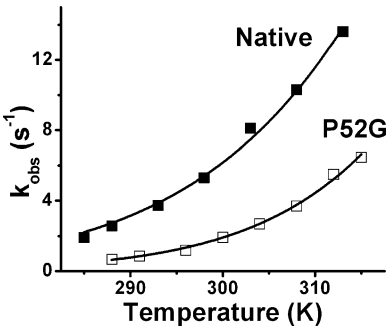

FIGURE 4: Effect of the P52G mutation on the ET reaction from reduced *O*-quinol MADH to oxidized amicyanin. The solid lines represent fits of the data to eq 5 for native (■) and P52G (□) amicyanin.

Table 4: Salt Dependence of the Reactions of *N*-Quinol MADH with Native and P52G Amicyanins

	N-quinol reaction rate (s^{-1})	
10 mM buffer containing	with P52G amicyanin	with native amicyanin[a]
0 mM KCl	4.1	42
50 mM KCl	13.1	
100 mM KCl	18.6	
150 mM KCl	19.7	
200 mM KCl	20.1	144
400 mM KCl		480

[a] Taken from ref 18 (*18*).

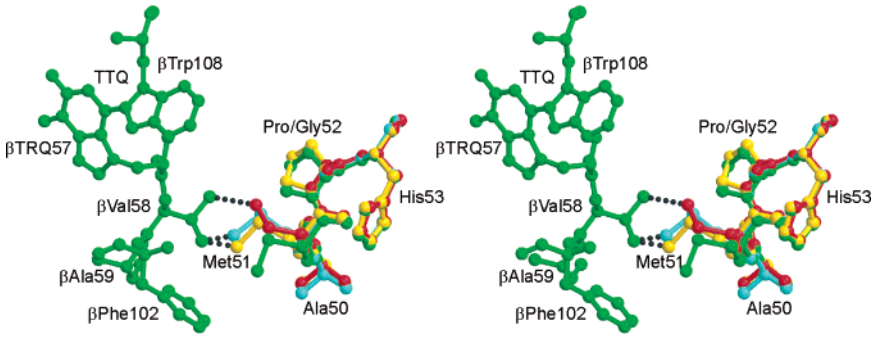

FIGURE 5: Interactions of native and P52G mutant forms of amicyanin with methylamine dehydrogenase. A portion of the observed interface between MADH and amicyanin showing residues βTRQ57, βVal58, βAla59, βPhe102, βTrp108, and residues Ala50−His53 of amicyanin in the crystal structure of the ternary complex of MADH with amicyanin and cytochrome *c*-551i is shown in a ball-and-stick format in green. Residues Ala50−His53 of the uncomplexed native amicyanin (yellow) and the oxidized (cyan) and reduced (red) P52G mutants of amicyanin are also shown in ball-and-stick format. The close contacts of atom Met51 CE with the side chain of βVal58 of MADH in the modeled complex are shown as black dotted lines ranging from 1.7 to 2.6 Å. This stereo diagram was prepared using Molscript (*45*) and reaster3D (*46*).

DISCUSSION

Structural Basis for Changes in Amicyanin−MADH Interactions. Both hydrophobic and electrostatic attractions are important in the interactions between native MADH and amicyanin (*21*). Hydrophobic residues that have been implicated to play a vital role at the binding interface of MADH and amicyanin include Met71, Met51, Met28, Pro52, Pro94, Pro96, and Phe97 of amicyanin. A significant role of Phe97 in stabilizing the complex was demonstrated by site-directed mutagenesis of this residue (*21*, *37*). Although the hydrophobic amino acid residues present at the interface move very little on complex formation, as judged by the crystal structures, the side chain of Asp180 of the MADH large subunit, which forms a salt bridge with Arg99 of amicyanin, exhibits significant rotation about its $C_\alpha-C_\beta$ bond. It was demonstrated by the site-directed mutagenesis of each of these two residues that this salt bridge accounts for the stabilization of the complex at low ionic strength and decreases the K_d value for the MADH−amicyanin complex at low ionic strength by about 100-fold (*21*, *38*). A model was proposed, where the hydrophobic interaction precedes the formation of the salt bridge between Asp180 and Arg99 (*38*). Initially, the desolvation of hydrophobic residues on protein association provides the driving force to stabilize the formation of the salt bridge; a slight shift in Asp180 and the electrostatic interaction with Arg99 further stabilizes complex formation by decreasing the off rate for the dissociation of the complex. An inspection of the P52G amicyanin structures suggest that these hydrophobic interactions are perturbed by the mutation.

The loss of three carbons of Pro52 in P52G amicyanin reduces the number of potential hydrophobic interactions in the amicyanin−MADH complex (Figure 2). This was quantified by carrying out the P52G mutation in silico using the crystal structure of the ternary complex determined at 1.9 Å resolution (pdb ID, 2GC4) and measuring the change in buried surface area as described in Experimental Procedures. The results indicate that the buried surface area of amicyanin in the complex is reduced from 783 to 764 Å^2 and of MADH from 725 to 710 Å^2, a drop of about 2.5%. It was also noted earlier that the side chain of Met51 of the oxidized P52G mutant is similarly oriented to that of the uncomplexed native amicyanin but quite differently from that of the reduced P52G structure. However, all three of these Met51 orientations differ considerably from that of amicyanin in complex with MADH (Figure 5). When the three native and P52G mutant amicyanin structures are modeled into the crystal structure of the MADH−amicyanin complex, atom C^ϵ of Met51 is found to make close contacts ranging from 1.7 to 2.6 Å with the side chain of βVal56 of MADH so that the reorientation of this side chain is necessary for complex formation. Thus, these two consequences of the P52G mutation, both of which contribute to the weakened hydrophobic interactions between amicyanin with MADH in the native complex, likely account for the observed increase in K_d for the of P52G amicyanin−MADH complex. These changes in structure and position of residues 51 and 52 may also account for the inability to crystallize the protein complexes with P52G amicyanin. The relevance of these apparent changes at the protein−protein interface to the interprotein ET reactions of these proteins is discussed later.

Physical and Redox Properties. The crystal structure of P52G amicyanin and its visible absorption and EPR spectra indicate that the copper coordination in P52G amicyanin is very similar to that of native amicyanin. The E_m value of free P52G amicyanin at pH 7.0 is 50 mV less positive than that of native amicyanin. However, an analysis of the pH dependence of the E_m value revealed that this decrease at neutral pH is due primarily to a shift in the pK_a value from 7.7 to 6.3, rather than a change in the electronic properties of the copper center. The pH dependence of the E_m value of free amicyanin describes the protonation of His95 in reduced amicyanin. When the side-chain of His95 becomes doubly protonated, it rotates by 180° about the $C_\beta-C_\gamma$ bond removing atom N^δ from the ligand sphere of copper (*11*). We have previously shown that mutations P94F and P94A of amicyanin shift the pK_a of the pH dependence of the E_m value to more acidic values because they introduce a steric hindrance to the rotation of His95 (*34*). An inspection of the structures of oxidized and reduced native and P52G amicyanin reveals no obvious basis for the shift in pK_a value caused by the P52G mutation. Water appears to be able to H bond to both the carbonyl oxygen of residue 52 as well as the His95 side chain, but it is not apparent that there is any differential stabilization of the different conformations of His95 in the mutant versus the native amicyanins. As

Scheme 1

$$A_{ox}\text{-}B_{red} \underset{k_{-X}}{\overset{k_X}{\rightleftharpoons}} [A_{ox}\text{-}B_{red}]^* \underset{k_{-ET}}{\overset{k_{ET}}{\rightleftharpoons}} A_{red}\text{-}B_{ox}$$

true ET:	$k_{ET} \ll k_X$	$K_X(k_X/k_{-X}) \gg 1$	$k_{obs} = k_{ET}$
gated ET:	$k_X \ll k_{ET}$		$k_{obs} = k_X$
coupled ET:	$k_{ET} \ll k_X$	$K_X(k_X/k_{-X}) \ll 1$	$k_{obs} = K_X * k_{ET}$

Scheme 2

$$A_{ox} + B_{red} \overset{K_d}{\rightleftharpoons} A_{ox}\text{-}B_{red} \underset{k_{-X}}{\overset{k_X}{\rightleftharpoons}} [A_{ox}\text{-}B_{red}]^* \underset{k_{-ET}}{\overset{k_{ET}}{\rightleftharpoons}} A_{red}\text{-}B_{ox}$$

Gating of rate-limiting ET from O-quinol MADH

$$A_{ox} + B_{red} \overset{K_d}{\rightleftharpoons} A_{ox}\text{-}B_{red} \underset{k_{-X}}{\overset{k_X}{\rightleftharpoons}} [A_{ox}\text{-}B_{red}]^* \underset{k_{-PT}}{\overset{k_{PT}}{\rightleftharpoons}} [A_{ox}\text{-}B_{red}]^{**} \underset{k_{-ET}}{\overset{k_{ET}}{\rightleftharpoons}} A_{red}\text{-}B_{ox}$$

Gating of rate-limiting PT from N-quinol MADH

discussed below, the proposed explanation for the changes in ET parameters that result from the P52G mutation include subtle and perhaps dynamic changes in the interactions of surface residues of amicyanin at the amicyanin−MADH interface. His95 also resides in this region of the protein, and it is possible that these changes in that region of the protein influence the relative stabilities of the different conformations of the His95 side chain such that it results in the observed shift in pK_a value.

Changes in ET Parameters. The correct interpretation of the basis of the change in a rate constant for an ET reaction that results from site-directed mutagenesis depends on whether the observed reaction is true, gated, or coupled ET (Scheme 1) (*39*, *40*). We have previously described approaches to distinguish between these possibilities by the analysis of the dependence of the observed ET rate constant on temperature and $\Delta G°$ (*18*, *36*, *39*, *41*). We have previously shown that under physiological conditions, the reaction of *O*-quinol MADH to amicyanin is a true ET reaction (*13*, *14*), whereas the ET reaction from *N*-quinol MADH to amicyanin is gated (*19*). The rate of the *N*-quinol reaction is that of the deprotonation of the *N*-quinol amino group, which is dependent on the presence of monovalent cations (*16*, *18*). The rate of this reaction is actually much greater than that of the *O*-quinol reaction because the deprotonation results in a highly reactive activated intermediate for ET (*18*).

The results obtained for the ET reactions of P52G amicyanin (Tables 3 and 4) indicate that the mutation has affected the rates of interprotein ET from both the *O*-quinol and *N*-quinol forms of MADH. Because different reaction steps are rate-limiting for the true ET reaction of the *O*-quinol and the gated ET reaction of the *N*-quinol, it appears that the P52G mutation has caused some reaction step that precedes both the true and gated ET reactions to now rate limit the overall reaction. A kinetic model to account for these observations is presented in Scheme 2, and the rationale for proposing this model is discussed below.

A possible explanation for these results is that the most stable equilibrium configuration of the complex of P52G amicyanin with MADH is not identical to that of native amicyanin with MADH. The observed change in K_d value for the complex caused by the mutation supports the notion that the protein−protein interface has been perturbed. If the configuration of the native complex is the one that is required for optimal interprotein ET, then for P52G amicyanin, a configurational rearrangement would be required to switch from a redox-inactive stable complex to a redox-active but unstable complex. Scheme 2 illustrates the impact of this additional reaction step on the kinetic mechanisms of the true ET from *O*-quinol amicyanin and the gated ET from *N*-quinol amicyanin.

For the reaction of P52G amicyanin with *O*-quinol MADH, both H_{AB} and λ increase relative to those of the true ET reaction with native amicyanin (Table 3). These parameters for P52G amicyanin do not likely describe a true ET reaction. An increase in H_{AB}, and a corresponding predicted decrease in ET distance, for true ET in this reaction is very unlikely because it is not really possible for the two redox centers to get any closer than they already are in the native complex. The changes in parameters likely mean that the configurational rearrangement has caused the overall ET reaction to become either coupled or gated. One cannot infer which one it is solely on the basis of the values of λ and H_{AB}. The conclusion that the reaction has become gated is supported by the results of the studies of the effect of the mutation on the reaction of the *N*-quinol MADH. The rates of the reactions of P52G amicyanin with the *O*-quinol and *N*-quinol are essentially identical in a 10 mM phosphate buffer. This suggests that K_x (k_x/k_{-x}) in Scheme 2 is not attenuating the true k_{ET} as in coupled ET, but that each reaction is now rate-limited by a common reaction step with the rate k_x. The most reasonable interpretation of these results is that the reaction of P52G amicyanin with *N*-quinol MADH is no longer gated by the cation-dependent proton transfer (PT) but is now also gated by this common preceding reaction step.

The conclusion that the reaction of P52G amicyanin with *N*-quinol MADH is rate-limited by a different reaction step than the PT step that gates the reaction with native amicyanin is also supported by the differences in the dependence of the reaction rates on [KCl] (Table 4). The rate of each reaction is salt-dependent, but the profiles of the salt dependences are different. The salt dependence of the reactions of P52G amicyanin with *N*-quinol MADH, which plateaus at about 150 mM KCl, likely reflects the salt dependence of the configurational rearrangement (k_x). This is not surprising because the protein−protein interface includes hydrophobic and electrostatic interactions (*21*). In contrast, the rate of reaction of native amicyanin with *N*-quinol MADH, which is the rate of the PT step, increases dramatically from 0 to 400 mM KCl (*18*).

Conclusion. The rationale for making the P52G mutation was to attempt to alter the ligand geometry of the type I site. Although this turned out not to be the case, the consequences of the P52G mutation have provided valuable new insights into the structural basis for the mechanisms of kinetic regulation of interprotein ET reactions. We had previously shown that the stability of the amicyanin−MADH complex depended upon a unique combination of hydrophobic and electrostatic interactions between residues from

each protein (*21*, *37*, *38*). We show here that the subtle perturbations of these protein−protein interactions also have significant effects on the rates of ET with the protein complex. These results suggest that surface residues of redox proteins likely evolved not only to dictate specificity for their redox protein partners but also to optimize the orientations of the redox centers and intervening media for the ET event.

ACKNOWLEDGMENT

We gratefully acknowledge Dr. William E. Antholine for his assistance in obtaining and interpreting the EPR spectra that were recorded at the National Biomedical ESR Center at the Medical College of Wisconsin, which is supported by NIH grant EB001980, Dr. James Hyde, PI.

REFERENCES

1. Husain, M., and Davidson, V. L. (1985) An inducible periplasmic blue copper protein from *Paracoccus denitrificans*. Purification, properties, and physiological role, *J. Biol. Chem. 260*, 14626−14629.
2. Adman, E. T. (1991) Copper protein structures, *Adv. Protein Chem. 42*, 145−197.
3. Durley, R., Chen, L., Lim, L. W., Mathews, F. S., and Davidson, V. L. (1993) Crystal structure analysis of amicyanin and apoamicyanin from *Paracoccus denitrificans* at 2.0 Å and 1.8 Å resolution, *Protein Sci. 2*, 739−752.
4. Cunane, L. M., Chen, Z., Durley, R. C. E., and Mathews, F. S. (1996) X-ray crystal structure of the cupredoxin amicyanin from *Paracoccus denitrificans*, refined at 1.31 Å resolution., *Acta Crystallogr., Sect. D 52*, 676−686.
5. Davidson, V. L. (2001) Pyrroloquinoline quinone (PQQ) from methanol dehydrogenase and tryptophan tryptophylquinone (TTQ) from methylamine dehydrogenase, *Adv. Protein Chem. 58*, 95−140.
6. Husain, M., and Davidson, V. L. (1986) Characterization of two inducible periplasmic *c*-type cytochromes from *Paracoccus denitrificans*, *J. Biol. Chem. 261*, 8577−8580.
7. Chen, L., Durley, R., Poliks, B. J., Hamada, K., Chen, Z., Mathews, F. S., Davidson, V. L., Satow, Y., Huizinga, E., and Vellieux, F. M. (1992) Crystal structure of an electron-transfer complex between methylamine dehydrogenase and amicyanin, *Biochemistry 31*, 4959−4964.
8. Chen, L., Durley, R. C., Mathews, F. S., and Davidson, V. L. (1994) Structure of an electron transfer complex: methylamine dehydrogenase, amicyanin, and cytochrome c551i, *Science 264*, 86−90.
9. Davidson, V. L., and Jones, L. H. (1995) Complex formation with methylamine dehydrogenase affects the pathway of electron transfer from amicyanin to cytochrome *c*-551i, *J. Biol. Chem. 270*, 23941−23943.
10. Gray, K. A., Davidson, V. L., and Knaff, D. B. (1988) Complex formation between methylamine dehydrogenase and amicyanin from *Paracoccus denitrificans*, *J. Biol. Chem. 263*, 13987−13990.
11. Zhu, Z., Cunane, L. M., Chen, Z., Durley, R. C., Mathews, F. S., and Davidson, V. L. (1998) Molecular basis for interprotein complex-dependent effects on the redox properties of amicyanin, *Biochemistry 37*, 17128−17136.
12. McIntire, W. S., Wemmer, D. E., Chistoserdov, A., and Lidstrom, M. E. (1991) A new cofactor in a prokaryotic enzyme: tryptophan tryptophylquinone as the redox prosthetic group in methylamine dehydrogenase, *Science 252*, 817−824.
13. Brooks, H. B., and Davidson, V. L. (1994) Kinetic and thermodynamic analysis of a physiologic intermolecular electron-transfer reaction between methylamine dehydrogenase and amicyanin, *Biochemistry 33*, 5696−5701.
14. Brooks, H. B., and Davidson, V. L. (1994) Free energy dependence of the electron transfer reaction between methylamine dehydrogenase and amicyanin, *J. Am. Chem. Soc. 116*, 11201−11202.
15. Bishop, G. R., and Davidson, V. L. (1998) Electron transfer from the aminosemiquinone reaction intermediate of methylamine dehydrogenase to amicyanin, *Biochemistry 37*, 11026−11032.
16. Bishop, G. R., and Davidson, V. L. (1995) Intermolecular electron transfer from substrate-reduced methylamine dehydrogenase to amicyanin is linked to proton transfer, *Biochemistry 34*, 12082−12086.
17. Davidson, V. L., Brooks, H. B., Graichen, M. E., Jones, L. H., and Hyun, Y. L. (1995) Detection of intermediates in tryptophan tryptophylquinone enzymes, *Methods Enzymol. 258*, 176−190.
18. Bishop, G. R., and Davidson, V. L. (1997) Catalytic role of monovalent cations in the mechanism of proton transfer which gates an interprotein electron transfer reaction, *Biochemistry 36*, 13586−13592.
19. Davidson, V. L., and Sun, D. (2003) Evidence for substrate activation of electron transfer from methylamine dehydrogenase to amicyanin, *J. Am. Chem. Soc. 125*, 3224−3225.
20. Davidson, V. L. (1990) Methylamine dehydrogenases from methylotrophic bacteria, *Methods Enzymol. 188*, 241−246.
21. Davidson, V. L., Jones, L. H., Graichen, M. E., Mathews, F. S., and Hosler, J. P. (1997) Factors which stabilize the methylamine dehydrogenase-amicyanin electron transfer protein complex revealed by site-directed mutagenesis, *Biochemistry 36*, 12733−12738.
22. Chistoserdov, A. Y., Boyd, J., Mathews, F. S., and Lidstrom, M. E. (1992) The genetic organization of the *mau* gene cluster of the facultative autotroph *Paracoccus denitrificans*, *Biochem. Biophys. Res. Commun. 184*, 1181−1189.
23. Lim, L. W., Mathews, F. S., Husain, M., and Davidson, V. L. (1986) Preliminary X-ray crystallographic study of amicyanin from *Paracoccus denitrificans*, *J. Mol. Biol. 189*, 257−258.
24. Otwinowski, Z., and Minor, W. (1997) Processing of X-ray diffraction data collected by oscillation methods, *Methods Enzymol. 276*, 307−326.
25. Sheldrick, G. M., and Schneider, T. R. (1997) SHELXL: High resolution refinement, *Methods Enzymol. 277*, 319−343.
26. CCP4. (1994) Collaborative computational project number 4, *Acta Crystallogr., Sect. D 50*, 760−763.
27. Kleywegt, G. J., and Jones, T. A. (1995) Where freedom is given, liberties are taken, *Structure 3*, 535−540.
28. Cammack, R. (1995) in *Bioenergetics: A Practical Approach* (Brown, G. C., and Cooper, C. E., Eds.) pp 85−109, IRL Press, New York.
29. Ma, J. K., Bishop, G. R., and Davidson, V. L. (2005) Role of the type I copper center in determining the stability of amicyanin, *Arch. Biochem. Biophys. 444*, 27−33.
30. Bishop, G. R., Brooks, H. B., and Davidson, V. L. (1996) Evidence for a tryptophan tryptophylquinone aminosemiquinone intermediate in the physiologic reaction between methylamine dehydrogenase and amicyanin, *Biochemistry 35*, 8948−8954.
31. Davidson, V. L., and Jones, L. H. (1996) Electron transfer from copper to heme within the methylamine dehydrogenase−amicyanin−cytochrome *c*-551i complex, *Biochemistry 35*, 8120−8125.
32. Marcus, R. A., and Sutin, N. (1985) Electron transfers in chemistry and biology, *Biochim. Biophys. Acta 811*, 265−322.
33. Morris, A. L., MacArthur, M. W., Hutchinson, E. G., and Thornton, J. M. (1992) Stereochemical quality of protein structure coordinates, *Proteins 12*, 345−364.
34. Carrell, C. J., Sun, D., Jiang, S., Davidson, V. L., and Mathews, F. S. (2004) Structural studies of two mutants of amicyanin from *Paracoccus denitrificans* that stabilize the reduced state of the copper, *Biochemistry 43*, 9372−9380.
35. Zhu, Z., and Davidson, V. L. (1998) Redox properties of tryptophan tryptophylquinone enzymes. Correlation with structure and reactivity, *J. Biol. Chem. 273*, 14254−14260.
36. Davidson, V. L. (2002) Chemically gated electron transfer. A means of accelerating and regulating rates of biological electron transfer, *Biochemistry 41*, 14633−14636.
37. Davidson, V. L., Jones, L. H., and Zhu, Z. (1998) Site-directed mutagenesis of Phe 97 to Glu in amicyanin alters the electronic coupling for interprotein electron transfer from quinol methylamine dehydrogenase, *Biochemistry 37*, 7371−7377.
38. Zhu, Z., Jones, L. H., Graichen, M. E., and Davidson, V. L. (2000) Molecular basis for complex formation between methylamine dehydrogenase and amicyanin revealed by inverse mutagenesis of an interprotein salt bridge, *Biochemistry 39*, 8830−8836.
39. Davidson, V. L. (1996) Unraveling the kinetic complexity of interprotein electron transfer reactions, *Biochemistry 35*, 14035−14039.
40. Davidson, V. L. (2000) Effects of kinetic coupling on experimentally determined electron transfer parameters, *Biochemistry 39*, 4924−4928.

41. Davidson, V. L. (2000) What controls the rates of interprotein electron-transfer reactions, *Acc. Chem. Res. 33*, 87−93.
42. Brünger, A. T. (1992) Free R-value: a novel statistical quantity for assessing the accuracy of crystal structures, *Nature (London) 355*, 472−475.
43. Luzzati, V. (1952) Traitment statistique des erreurs dans la determination des structures cristallines, *Acta Crystallogr. 5*, 802−810.
44. Cruickshank, D. W. I. (1999) Remarks about protein structure precision, *Acta Crystallogr., Sect. D 55*, 583−601.
45. Kraulis, P. J. (1991) MOLSCRIPT: a program to produce both detailed and schematic plots of protein structures, *J. Appl. Crystallogr. 24*, 946−950.
46. Merritt, E. A., and Bacon, D. J. (1997) Raster 3D: photorealistic molecular graphics, *Methods Enzymol. 277*, 505−524.

BI0605134